Blazar Modeling and the Minimum Power Condition

23 September 2016

Ruhr Astroparticle and Plasma Physics Inauguration Conference

Bochum, Germany

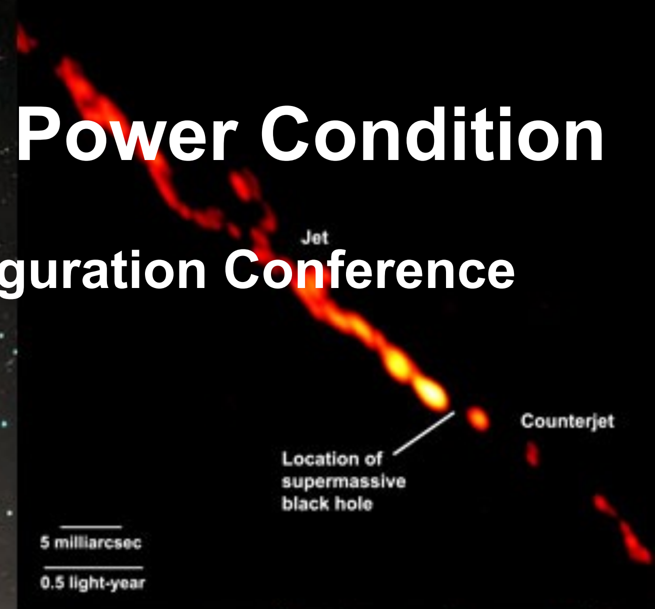

γ rays	IGMF
UHECRs	BH/jet physics
ν	SMBH growth and galaxy evolution
EBL	

Dr. Charles D. Dermer
George Mason University
Fairfax, Virginia USA

Blazars: Supermassive Black Holes with Relativistic Jets Pointed at Us

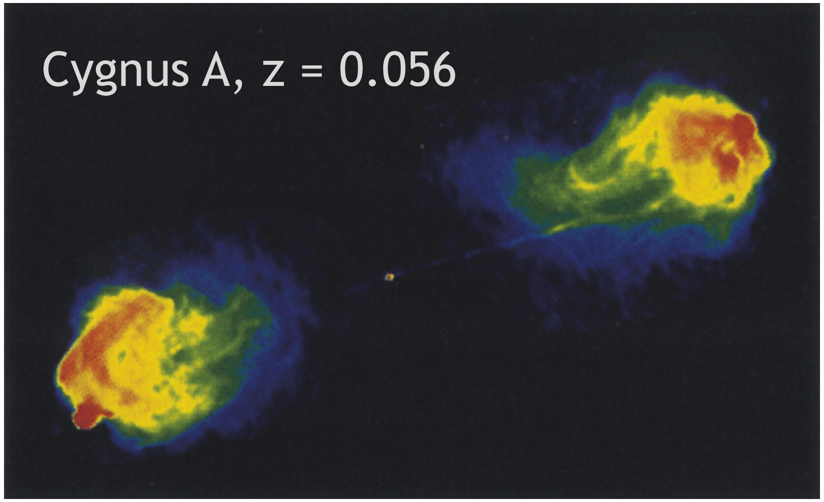

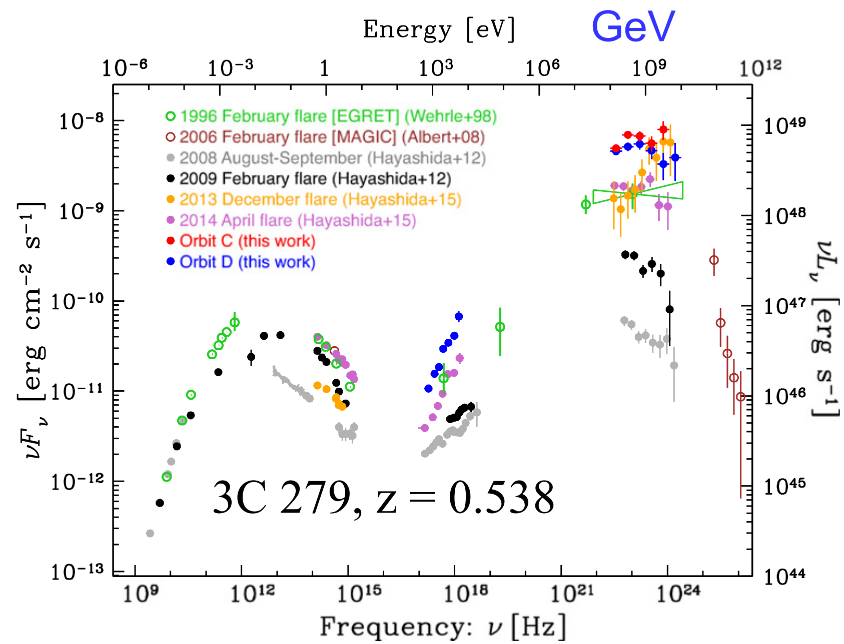

Causality argument for size of emission region

$$R / c \le \Delta t_{\rm var} \qquad R_S = \frac{2GM}{c^2} = 3\times 10^9 (M/M_9)\ cm \qquad L_{Edd} \approx 10^{47} (M/M_9)\ erg/s$$

$$\Delta t_{\rm var} \le 1\ day \qquad R_S / c \cong 10^4 (M/M_9)\ s \qquad L_{iso} \approx 10^{48} (M/M_9)\ erg/s$$

Puzzle of hyper-variable blazars

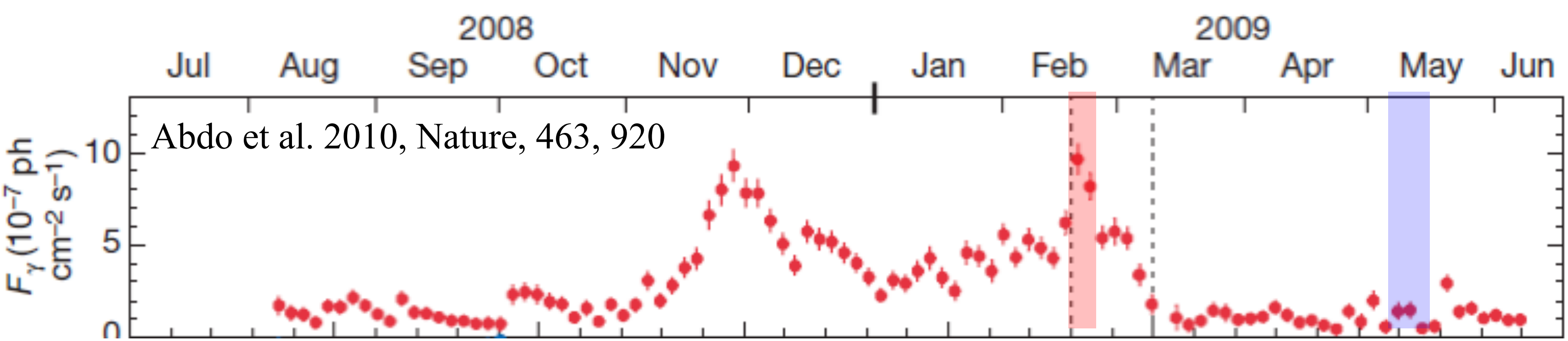

Classes of Active Galactic Nuclei and Unification

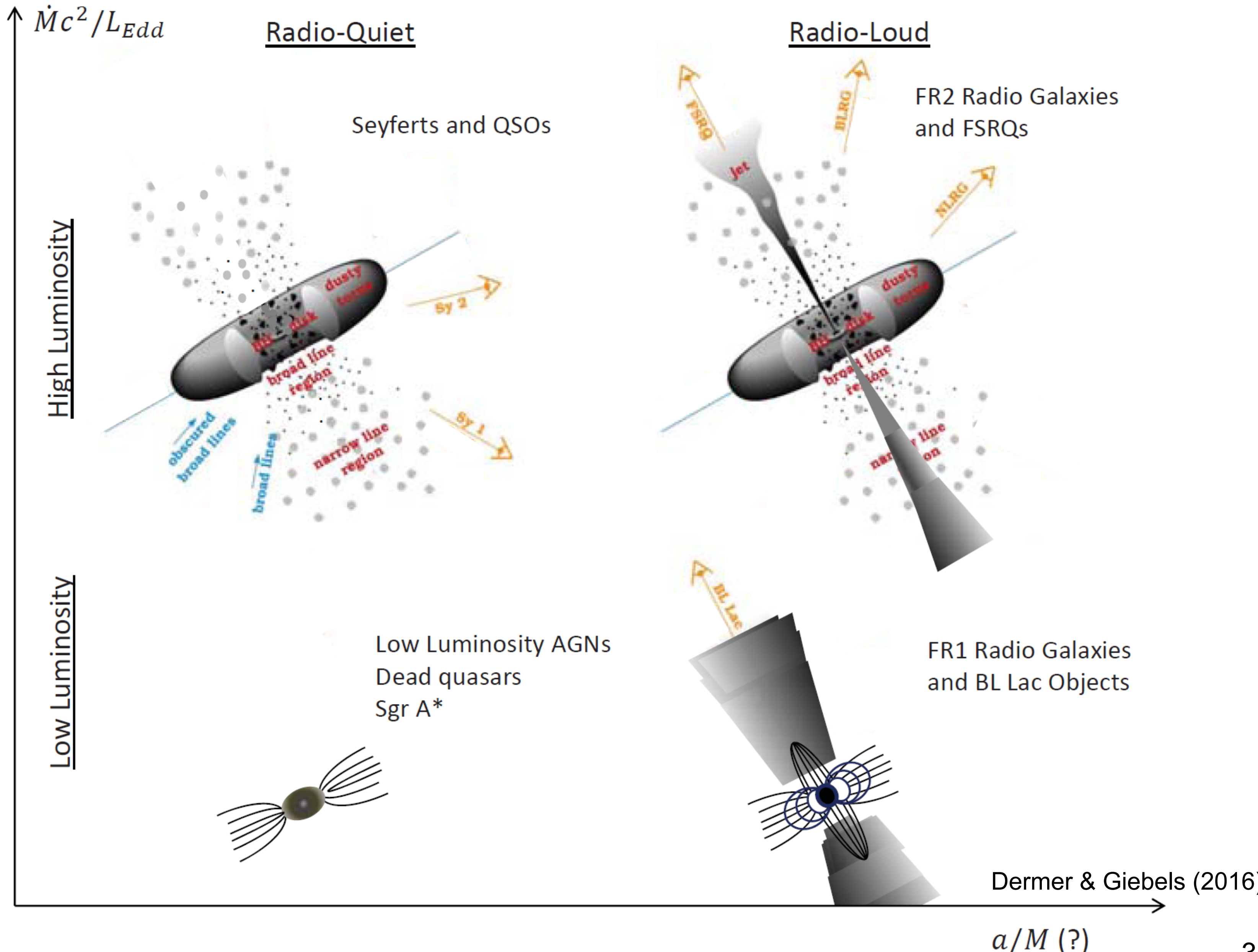

Blazar spectral energy (power) distributions

BL Lacs: emission to VHE/TeV energies

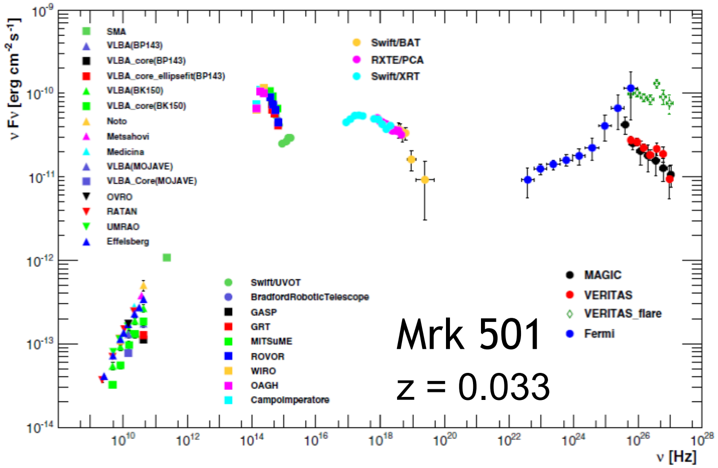

Abdo et al. 2011a

Abdo et al. 2011b

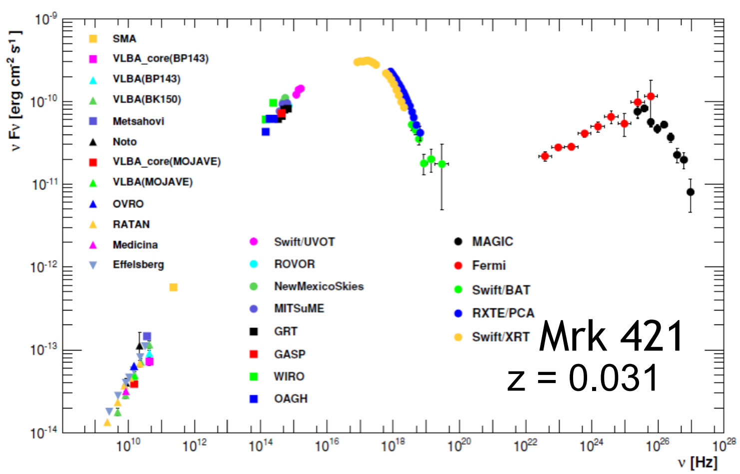

FSRQs: cutoffs at GeV with VHE episodes

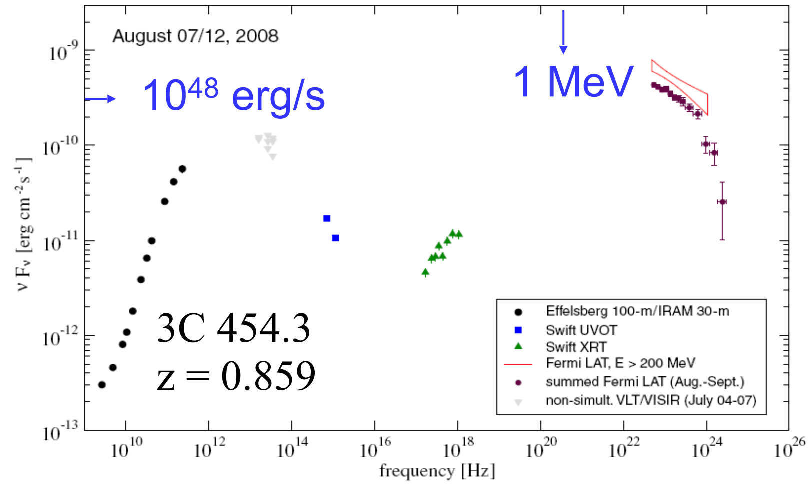

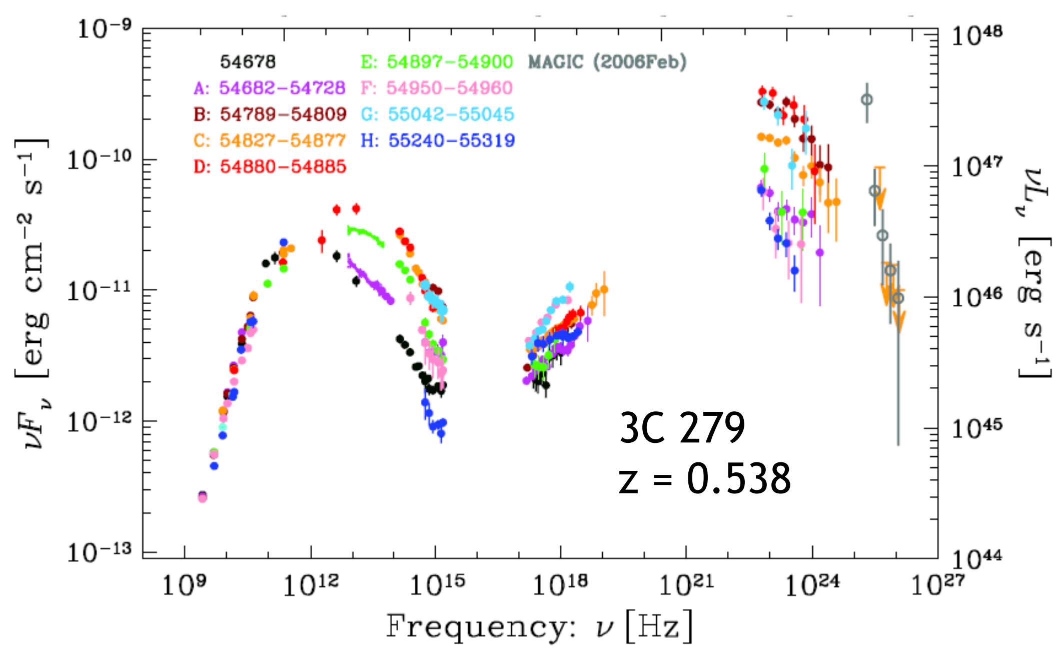

Two-humped SED

Blazar Modeling

Nonthermal γ rays ⇒ relativistic particles + intense photon fields

Leptonic jet models:

- Nonthermal synchrotron radiation for radio through optical (low-energy hump)
- Compton scattering of ambient radiation fields by jet electrons making high-energy X-ray/γ-ray component by synchrotron self-Compton **(SSC)** or external Compton (**EC**) processes (**FSRQs**)

Lepto-Hadronic jet models:

- Nonthermal synchrotron radiation for radio through optical (low-energy hump)
- Secondary nuclear production

  $\mathbf{p+N \rightarrow \pi^{o}, \pi^{\pm} \rightarrow \gamma, \nu, n, e^{\pm}}$
- Proton and ion synchrotron radiation

  $\mathbf{p+B \rightarrow \gamma}$
- Photomeson production

  $\mathbf{p\gamma \rightarrow \pi^{o}, \pi^{\pm} \rightarrow \gamma, \nu, n, e^{\pm}}$

Hadrons escape to become UHECRs

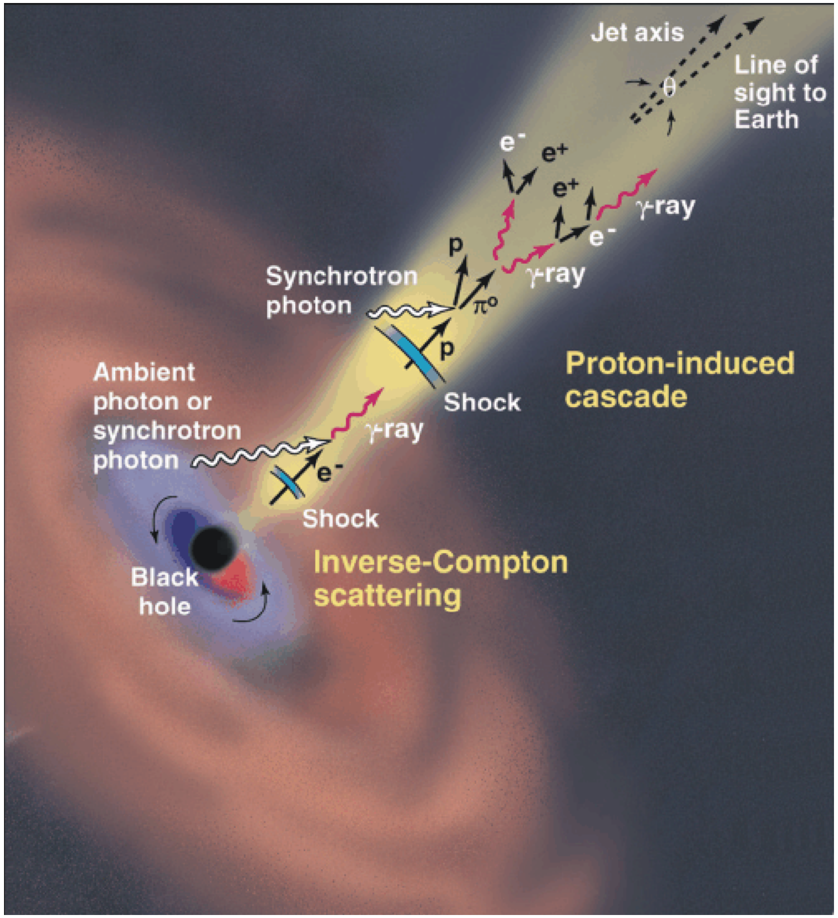

Particle Acceleration and Radiation in Leptonic Blazar Models

$$f_\varepsilon = \nu F_\nu$$

$$\frac{\partial n(\gamma;t)}{\partial t} + \frac{\partial}{\partial \gamma}[\dot{\gamma}\, n(\gamma;t)] + \frac{n(\gamma;t)}{t_{esc}(\gamma,t)} = \dot{n}(\gamma;t)$$

The synchrotron flux is then given by

$$f_\epsilon^{\rm syn} = \frac{\delta_{\rm D}^4 \epsilon' J'_{\rm syn}(\epsilon')}{4\pi d_L^2} = \frac{\sqrt{3}\delta_{\rm D}^4 \epsilon' e^3 B}{4\pi h d_L^2} \int_1^\infty d\gamma' N'_e(\gamma') R(x).$$

$$f_{\epsilon_s}^{\rm SSC} = \left(\frac{3}{2}\right)^3 \frac{d_L^2 \epsilon_s'^2}{R_b'^2 c \delta_{\rm D}^4 U_B} \int_0^\infty d\epsilon' \frac{f_{\tilde{\epsilon}}^{\rm syn}}{\epsilon'^3} \times \int_{\gamma'_{\rm min}}^{\gamma'_{\rm max}} d\gamma' \frac{F_{\rm C}(q,\Gamma_e) f_{\tilde{\epsilon}}^{\rm syn}}{\gamma'^5},$$

$$f_\epsilon^{EC} = \frac{3}{4} \frac{c\sigma_{\rm T}\epsilon_s^2}{d_L^2} \delta_{\rm D}^3 \int_0^\infty d\epsilon_* \frac{u_*(\epsilon_*)}{\epsilon_*^2} \int_{\gamma_{min}}^{\gamma_{max}} d\gamma \frac{N'_e(\gamma',\Omega')}{\gamma^2} F_{\rm C}(q,\Gamma_e)$$

1. Relativistic outflows
2. Single zone; exclude radio
3. Synchroton, SSC, and EC
4. Electron energy distribution
5. Power-law injection + losses
6. Nonlinear losses
7. Adiabatic expansion
8. Light travel-time effects
9. Cascading/$\gamma\gamma$ pairs in source and IGM
10. Multizone/spine-sheath
11. Anisotropic effects
12. Reverberation/echo

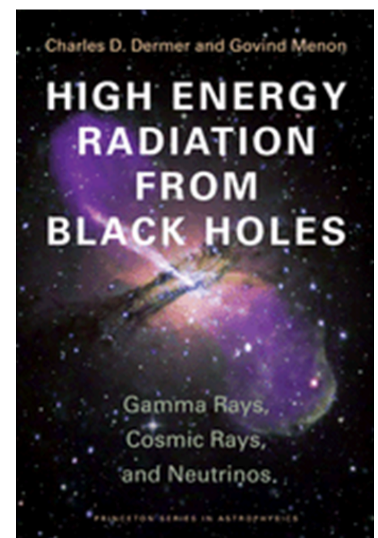

Boettcher & Chiang (2002)
Finke et al. (2008)
Dermer & Menon (2009)

Trend toward increasing complexity in blazar modeling

Spectrum and Jet Physics

- BL Lacs: synchrotron/SSC model fits

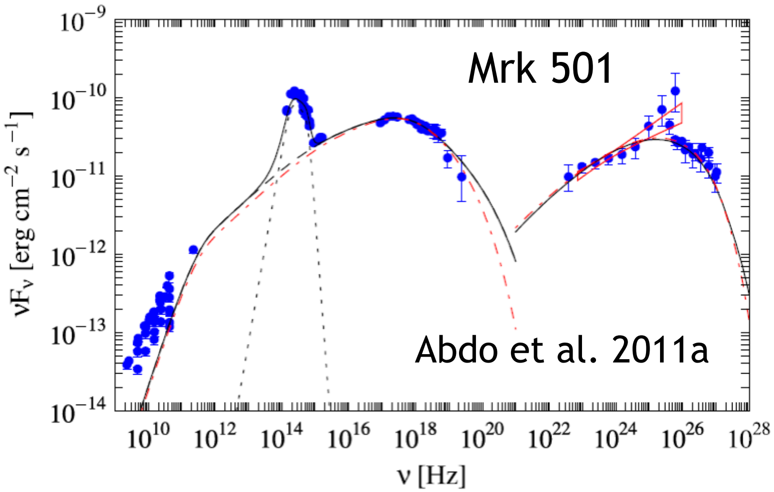

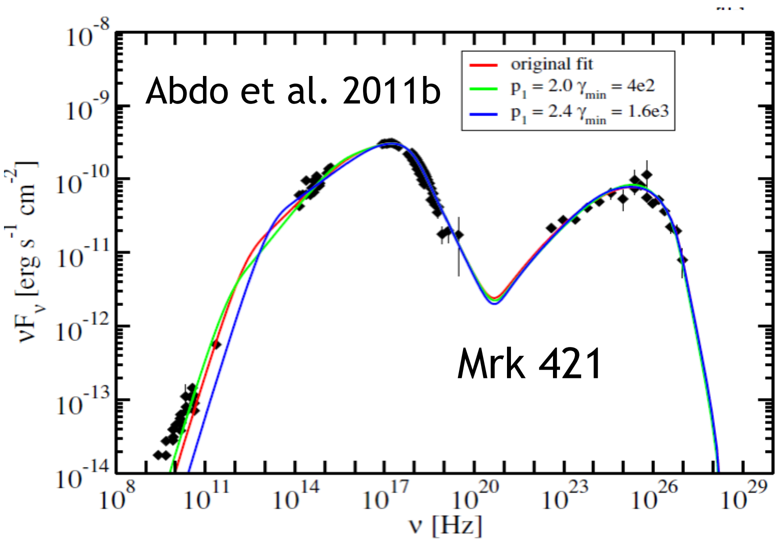

Multiple parameters: non-uniqueness

- FSRQs: synchrotron/SSC + EC

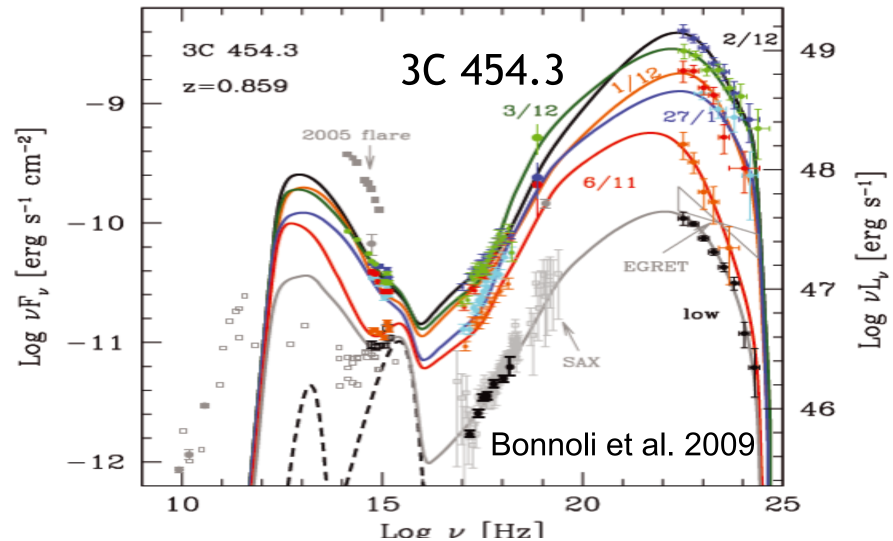

3C279

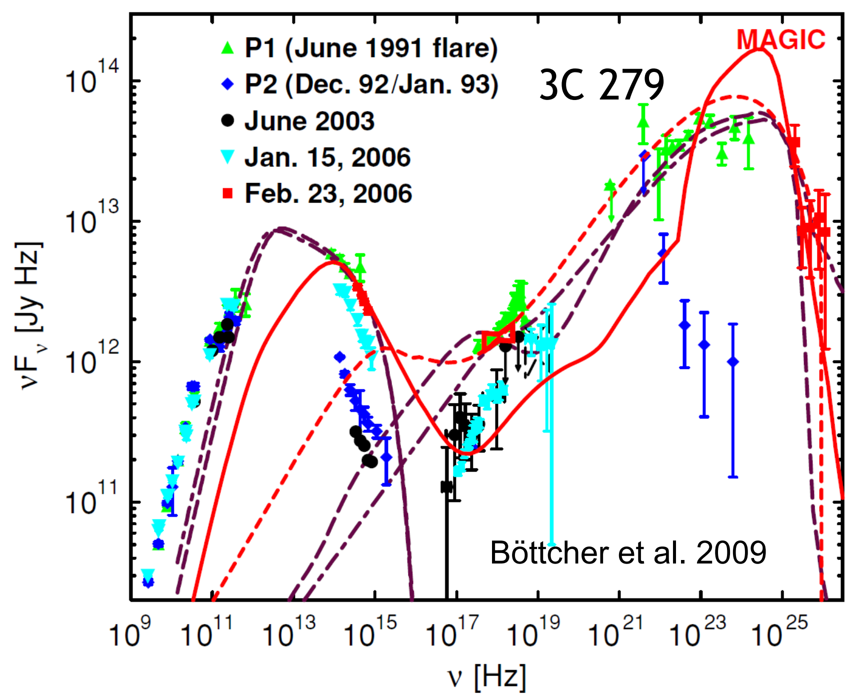

The Synchrotron Puzzle

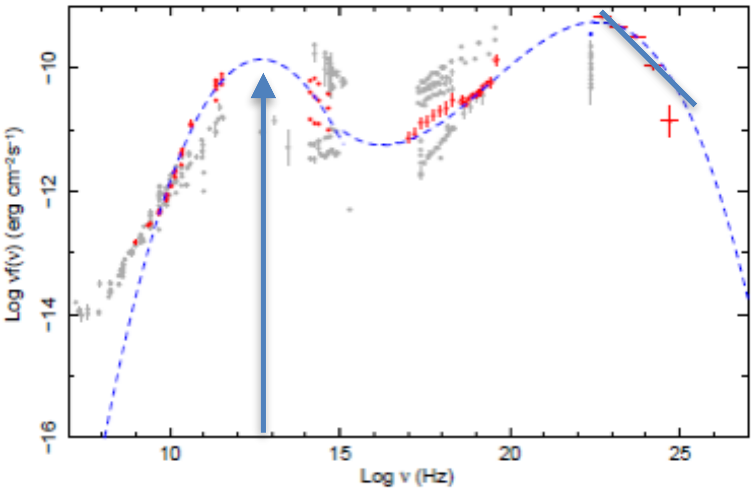

γ-ray photon index vs. peak synchrotron frequency

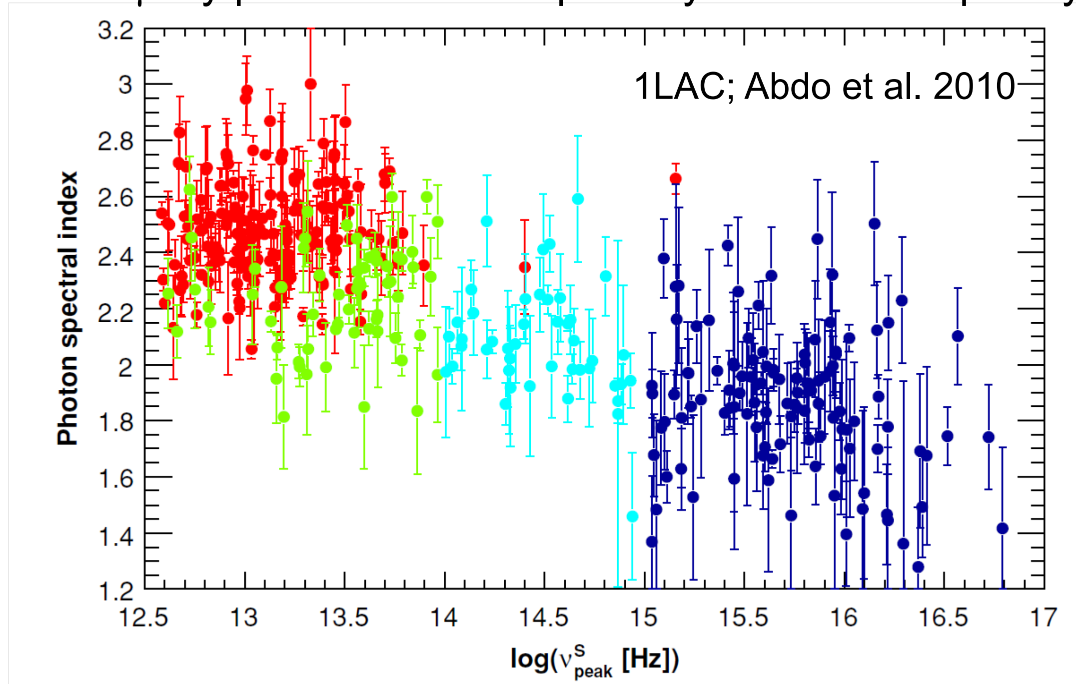

In Fermi acceleration scenarios, acceleration timescale > Larmor timescale

Equating synchrotron energy loss time scale with Larmor timescale implies maximum synchrotron energy ~ 100Γ MeV (de Jager & Harding 1992)

Peak or maximum synchrotron frequency of blazars 4-7 orders of magnitude less than theoretical maximum

Acceleration Physics and the Electron Energy Distribution

First-Order Fermi Acceleration

(Naively) makes power-law distributions $\gamma'^2 N'_e(\gamma'^2) \approx K(\frac{\gamma'}{\gamma'_{pk}})^{2-(\frac{2+r}{r-1})} = K(\frac{\gamma'}{\gamma'_{pk}})^{(\frac{r-4}{r-1})}$

Second-order Fermi Acceleration

$$t_{II} \propto \varsigma\beta_A^2\gamma^{2-q} \qquad \gamma'^2 N'_e(\gamma'^2) = K(\frac{\gamma'}{\gamma'_{pk}})^{-b\log(\gamma'/\gamma'_{pk})}$$

Makes curved log-parabola-like particle distribution
(Massaro et al. 2004; Stawarz & Petrosian 2008; Tramacere et al. 2007, 2011)

Fermi 1: separate acceleration and radiation regions
Fermi 2: acceleration and radiation regions same

Turbulent particle acceleration and magnetic reconnection invoked in highly magnetized jets for short variability time scales
(Lazarian et al.; Sironi & Spikovsky 2014; Giannios et al. 2009, Sironi, Petropoulou, & Giannios 2015)

Bright Fermi blazars explained by broken power-law and log-parabola spectral functions about equally (Kohler & Nalewajko 2015)

Blazar modeling with log-parabola electron energy distributions

CD, Yan, Zhang, Finke, Lott; ApJ 2015

Explain correlations of spectral index with peak synchrotron and Compton frequencies in blazars

$$\Gamma_\gamma = d - k \log \nu_{14}$$

$$\nu_{14} = \nu_s / 10^{14}\, Hz$$

$$k = 0.18 \pm 0.03$$

Spectral Index Diagram

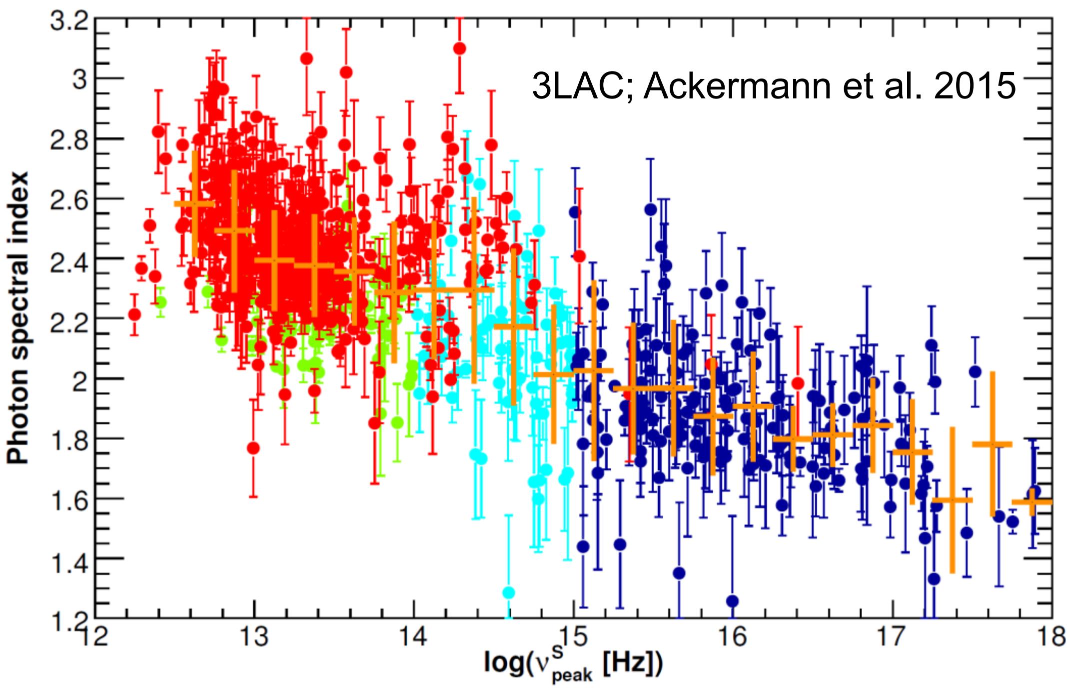

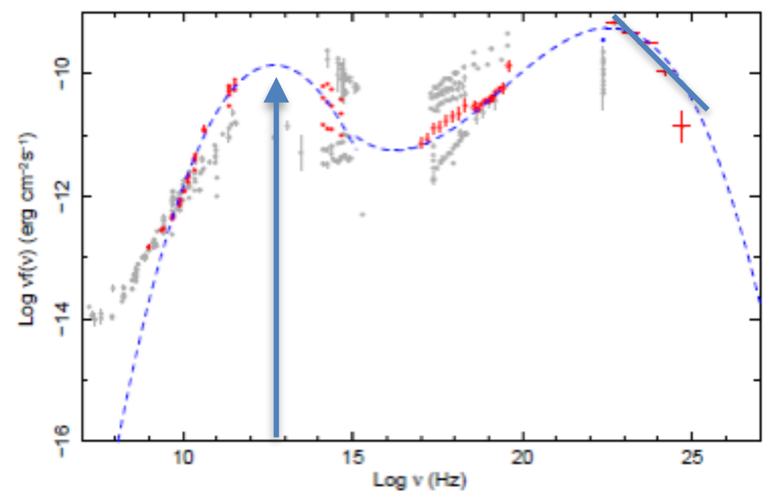

Near-equipartition, log-parabola model

Electron energy distribution (EED): $\gamma'^2 N'_e(\gamma') = K' y^{-b \log y}, \; y = \gamma'/\gamma'_{pk}$

Simplest non-trivial 3 parameter EED

b is log parabola width parameter

$$u'_{\rm syn} \;=\; L_{\rm syn}/4\pi r'^2_b c \delta^4_{\rm D} f_0 \qquad r'_b \cong c\delta_{\rm D} t_{\rm var}$$

kinematic

$$L_{\rm syn} = 4\pi t^2_{\rm var} c^3 \delta^6_{\rm D} u'_{\rm syn} f_0$$

lum

$$L_{\rm syn} = \frac{4}{3} c\sigma_{\rm T} u'_{B'} N_{e0} \gamma'^2_{\rm pk} \delta^4_{\rm D}$$

Equipartition relation:

$$u'_e = \frac{\mathcal{E}'_e}{V'_b} = \frac{m_e c^2 N_{e0} \gamma'_{\rm pk}}{V'_b} f_1 = \zeta_e u'_B$$

$$\delta_{\rm D} \cong 17.5 L_{48}^{3/16} \frac{\zeta_e^{1/4}}{\zeta_s^{7/16}} \frac{\nu_{14}^{1/8}}{t_4^{1/8}}$$

$$B'({\rm G}) \cong \frac{5.0\, \zeta_s^{13/16}}{L_{48}^{1/16} t_4^{5/8} \nu_{14}^{3/8} \zeta_e^{3/4}}$$

$$\gamma'_{\rm pk} \cong 523 \frac{\nu_{14}^{5/8} \zeta_e^{1/4}}{L_{48}^{1/16} \zeta_s^{3/16}} t_4^{3/8}$$

Dermer, Cerruti, Lott, Boisson, Zech 2014

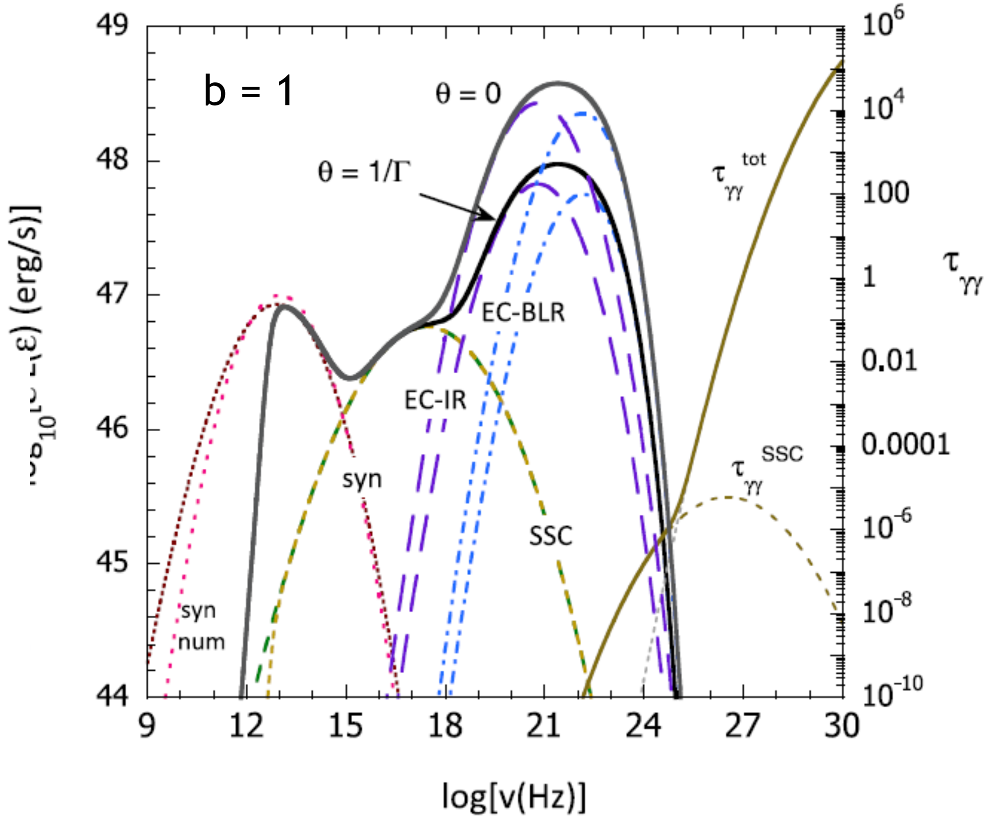

Completely solvable system; obtain external radiation field energy densities in FSRQ analysis

Equipartition modeling

$$L_{syn}^{pk}, \nu_{syn}^{pk}, t_{var} \Rightarrow B', \delta_D, R'$$

modulo b (from SED)
ζ_s (from SED modeling)
ζ_e (equipartition assumption; from SED modeling)

Data of Hayashida et al. (2012) on 3C 279
GeV break in LSPs, ISPs (Cerruti et al. 2013)
Models close to equipartition

TABLE 1
Dependences of δ_D, B', and $\gamma'_{]pk}$ [a]

	Coef.	L_{48}	ν_{14}	t_4	ζ_s	ζ_e	f_0	f_1	f_2
δ_D	17.5	3/16	1/8	−1/8	−7/16	1/4	−7/16	−1/4	−1/8
B'(G)	5.0	−1/16	−3/8	−5/8	13/16	−3/4	13/16	3/4	3/8
γ'_{pk}	523	−1/16	5/8	3/8	−3/16	1/4	−3/16	−1/4	−5/8
$\mathcal{E}^b$	1.4	5/16	−1/8	1/8	−1/16	−1/4	−11/16	1/4	1/8
$L^c_{jet,B}$	2.5	5/8	−1/4	1/4	−1/8	−1/2	−1/8	1/2	1/4

[a] So, e.g., $\delta_D \cong 17.5 L_{48}^{3/16}(\nu_{14}/f_2 t_4)^{1/8}(f_0\zeta_s)^{-7/16}(\zeta_e/f_1)^{1/4}$, etc.
[b] $\mathcal{E} = E_{max}(10^{20}\ eV)/Z$
[c] Absolute power in magnetic field, units of 10^{45} erg s^{-1}

Dermer et al. 2014

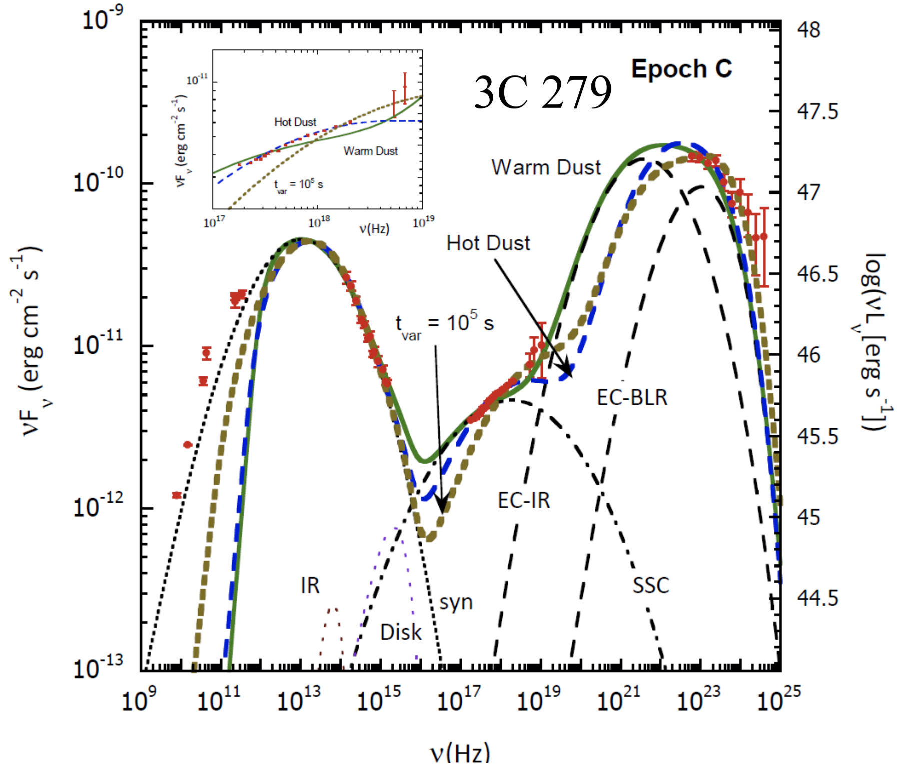

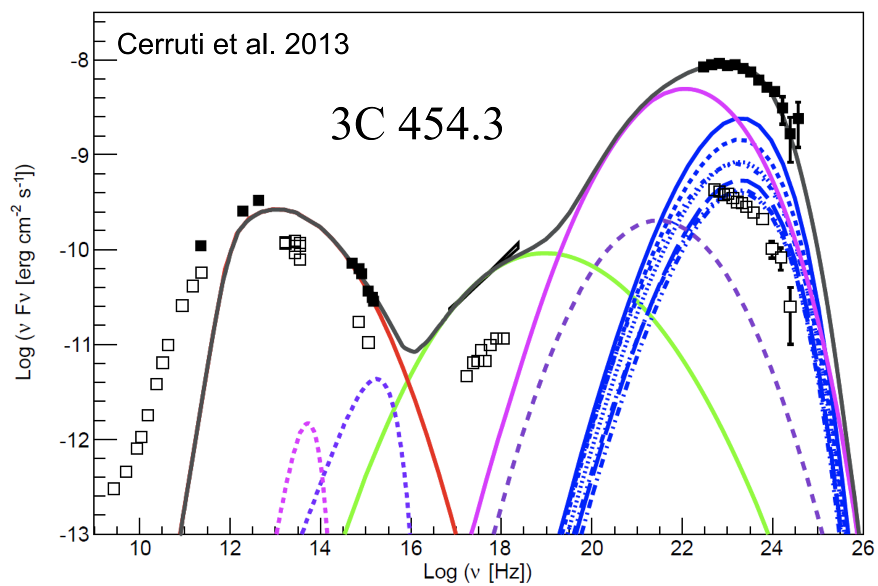

Analytic form for Spectral Index Diagrams

$$\gamma'^2 N'_e(\gamma') = K' y^{-b\log y},\ y = \gamma'/\gamma'_{pk}$$

The comoving synchrotron luminosity

$$L'_{syn} = c\sigma_{\rm T}\frac{B'^2}{6\pi}\int_1^\infty d\gamma'\gamma'^2 N_e(\gamma') \qquad \varepsilon_{pk} = \varepsilon_{pk,syn} = \delta_D \frac{4}{3}\frac{B'}{B_{cr}}\gamma'^2_{pk}$$

Results in Thomson regime

$$\epsilon L_{syn}(\epsilon) = \upsilon x^{1-\hat{b}\ln x} = \upsilon\left(\frac{\epsilon}{\epsilon_{pk}}\right)^{\frac{1}{2}-\frac{b}{4}\log(\epsilon/\epsilon_{pk})}$$

$$x = \sqrt{\epsilon/\epsilon_{pk}}$$
$$\upsilon = f_3 L_{syn}$$
$$f_3 = 10^{-1/4b}/(2\sqrt{\pi\ln 10/b})$$

(Dermer et al. 2014)

$$\alpha_\nu \equiv \frac{d\ln[\varepsilon L_{syn}(\varepsilon)]}{d\ln\varepsilon} = \frac{1}{2}[1 - b\log(\frac{\varepsilon}{\varepsilon_{pk}})]$$ (Massaro et al. 2004)

$$b_{sy} \cong \frac{b}{4}$$ (Massaro et al. 2006)

$$b_{SSC} \cong \frac{b}{8}$$ (Paggi et al. 2009)

$$\Gamma_\gamma^{EC} = \frac{17}{8} + \frac{b}{2}\log\left(\frac{f_0^{5/4}E_{GeV}\zeta_s^{5/4}}{\epsilon_{Ly\alpha}t_4^{1/2}\zeta_e L_{48}^{1/4}}\right) - \frac{3b}{4}\log\nu_{14}$$

$$\Gamma_\gamma^{SSC} = \frac{65}{32} + \frac{b}{4}\log\left(\frac{6.5\times 10^3 E_{GeV} f_0^{3/8}\zeta_s^{3/8}L_{48}^{1/8}}{\zeta_e^{1/2}t_4^{3/4}}\right) - \frac{9b}{16}\log\nu_{14}$$

By binning results according to b from synchrotron SED fit, identify radiation process

Equipartition Model vs. Synchrotron Spectral Index Diagram

$$b = 1/2,\ L_{48} = t_4 = \varsigma_s = \varsigma_e = E_{GeV} = 1$$

Slope for EC processes:

$$k_{EC} = \frac{3b}{4}$$

Slope for SSC processes:

$$k_{SSC} = \frac{9b}{16}$$

Three γ-ray emitting processes: SSC, EC BLR, EC IR

- **External radiation field densities:**

Ly alpha: 0.01 erg/cm^3

IR torus: 10^{-3} erg/cm^3; 1000 K dust

- **Compton dominance restricts EC, SSC regimes**
- **Double-headed arrow shows slope of +1 for Compton dominance (in Thomson regime)**

2LAC data: Red: FSRQ; Blue: BL Lac w/ z; Green: BL Lac w/o z

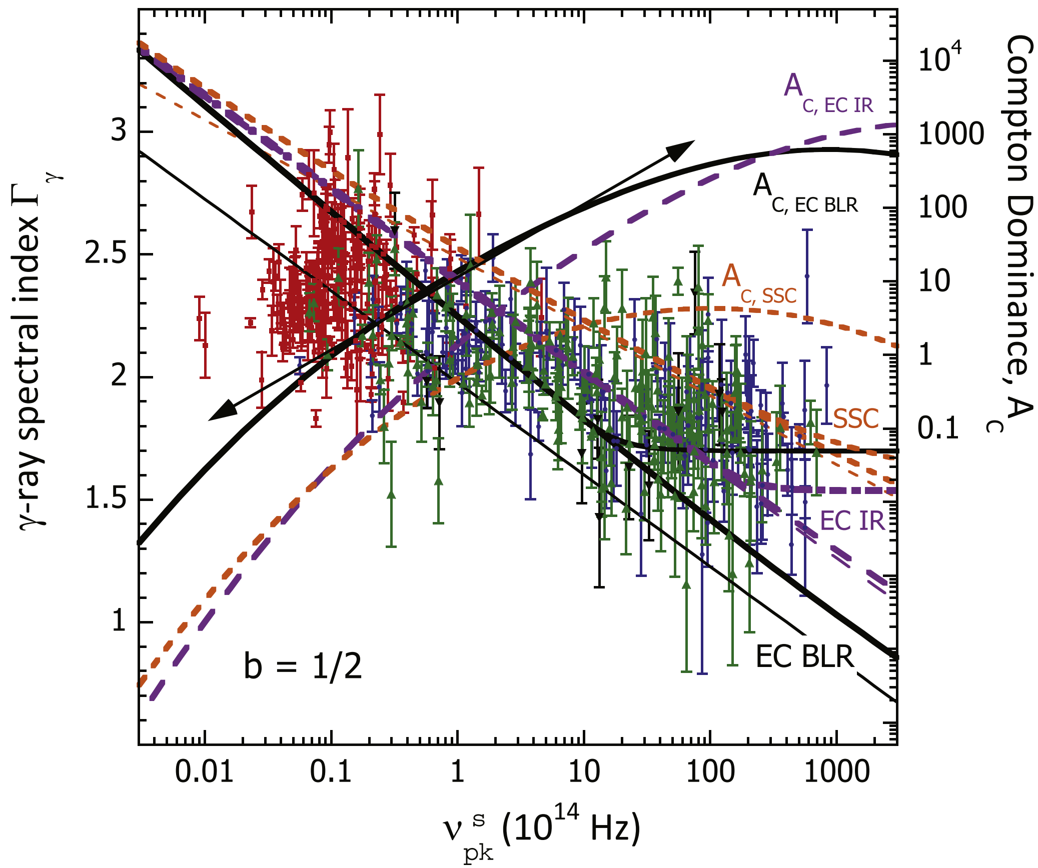

Equipartition model and γ-ray spectral index diagrams

Discriminate between SSC and EC processes in blazars

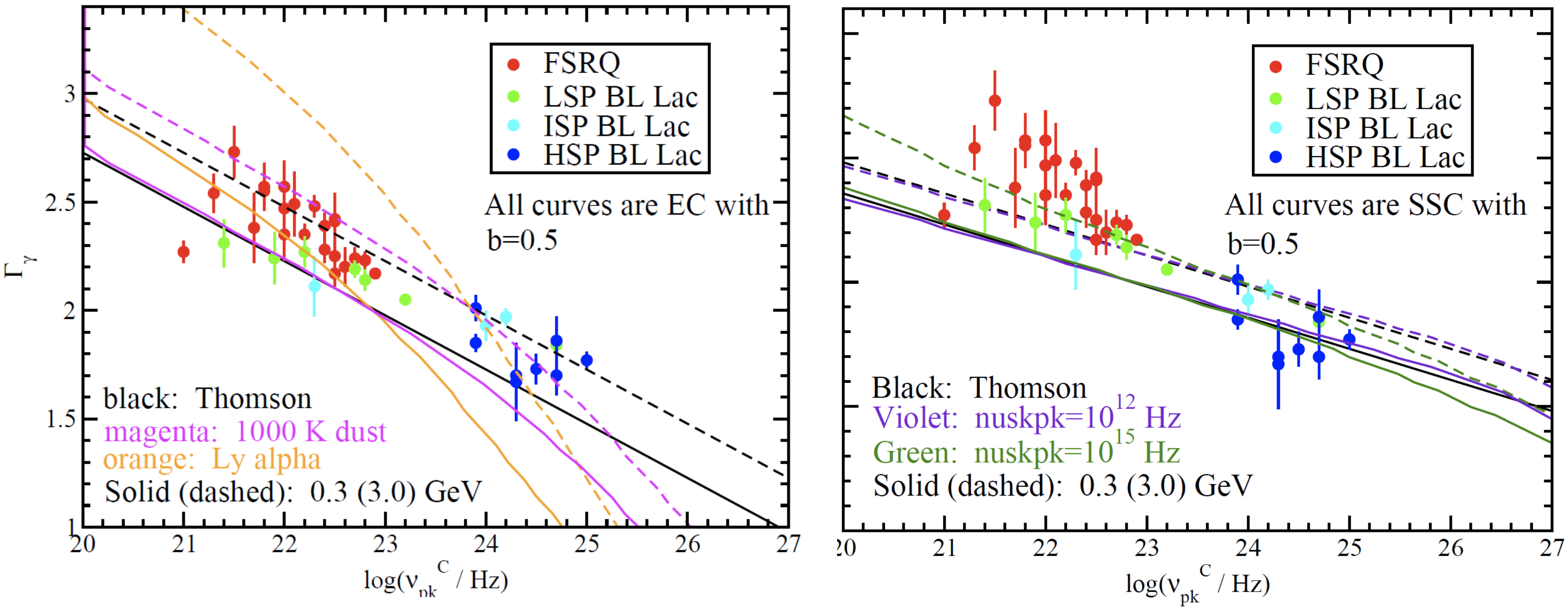

Thomson-regime expressions:

$$\Gamma_\gamma^{EC,\gamma} = 2 + \frac{b}{2}\log(2.4E_{GeV}) - \frac{b}{2}\log\nu_{23}$$

$$\Gamma_\gamma^{SSC,\gamma} = 2 + \frac{b}{4}\log(2.4E_{GeV}) - \frac{b}{4}\log\nu_{23}$$

Rules out SSC as a process for making γ-rays from FSRQs

Departures from equipartition: the case of Mrk 501

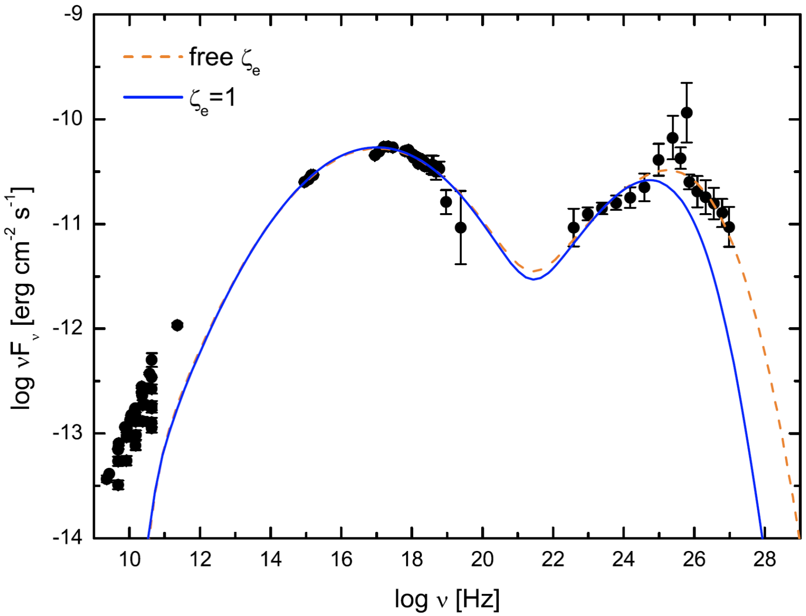

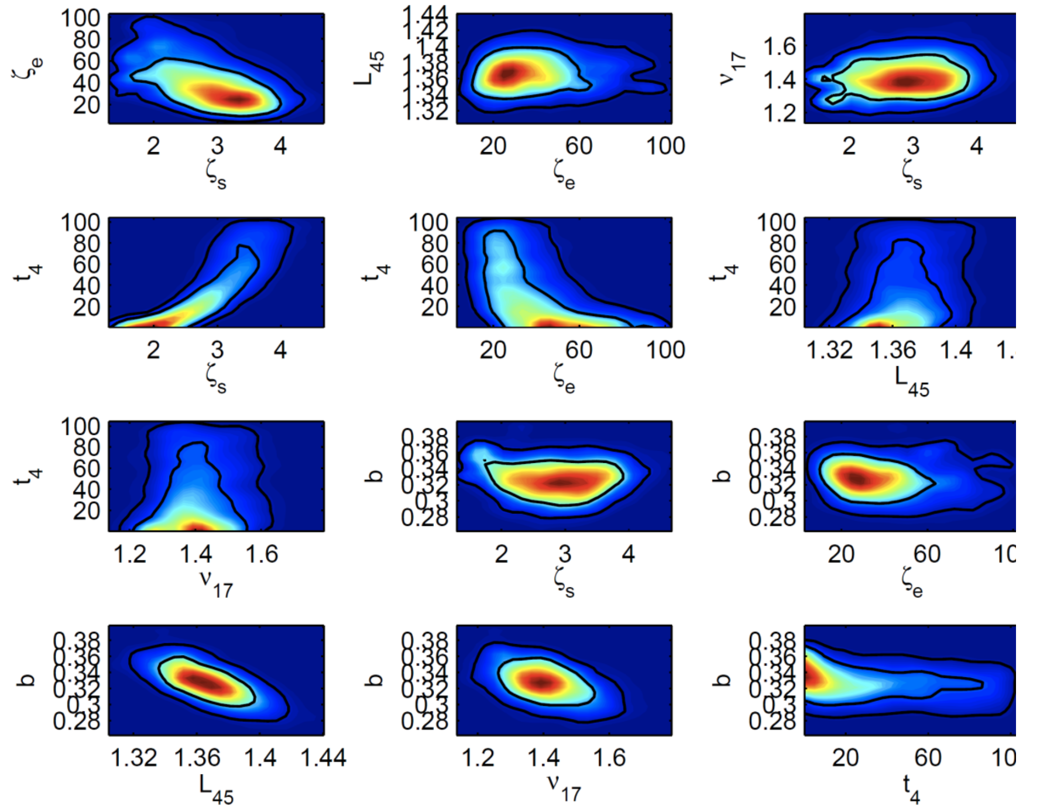

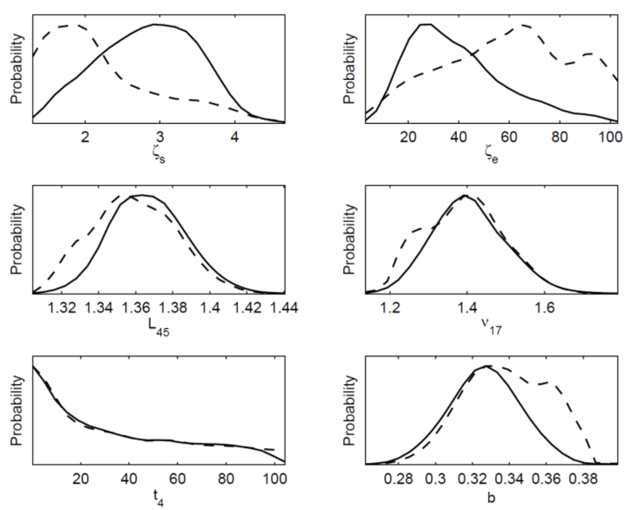

Use ζ_s and ζ_e for spectral-index modeling

Markov Chain Monte Carlo method (Lewis & Bridle 2002; Yuan et al. 2011; Liu et al. 2012)

Applied to Mrk 421 (Yan et al. 2013) and Mrk 501 (Peng et al. 2014) using different electron energy distributions

Blazar can be far from equipartition

Blazar modeling minimizing jet power

work with Maria Petropoulou (Purdue University): ApJL, 2016

Power analysis: $$L_j = 2\pi r_b'^2 \beta\Gamma^2 c \sum_{i=B,e,p} (u_i' + P_i') + L_j^r + L_j^{\rm cold}$$

$$u'_{B'} = B'^2/8\pi \qquad L_j^r = \kappa L_{\rm s,e}\psi^2/\delta_{\rm D}^2$$

$$u_i' = 3m_i c^2 \bar{\gamma}_i' N_i/4\pi r_b'^3 \qquad \psi \equiv 1 + (\Gamma\theta)^2 > 1$$

Minimize power with respect to magnetic field and Doppler factor for monoenergetic particle distributions

Leptonic synchro-Compton (LSC) jet models:

- Obtain unique results for magnetic field and Doppler factor from observables

$$B'_{\rm min} = 0.17\ \kappa^{-13/16} t_{v,3}^{-5/8} \epsilon_{-3}^{-3/8} L_{45}^{-1/16}\ {\rm G}$$

$$\delta_{\rm D,min} = 59.3\ \kappa^{7/16} L_{45}^{3/16} \epsilon_{-3}^{1/8} t_{v,3}^{-1/8}$$

Lepto-Hadronic synchrotron (LHS) jet models:

- Characterize acceleration efficiency through Hillas condition

$$B'_{\rm min} = 147\ \kappa^{-4/7} \eta^{3/7} t_{v,3}^{-4/7} L_{45}^{-4/7} L_{\gamma,45}^{3/7}\ {\rm G}$$

$$\delta_{\rm D,min} = 6.9\ \kappa^{5/14} \eta^{-1/7} L_{45}^{5/14} t_{v,3}^{-1/7} L_{\gamma,45}^{-1/7}$$

Derived blazar properties minimizing jet power

$$\text{Nominal values:} \quad L_{45} = t_{v,3} = \kappa = 1$$

Leptonic Blazar Model

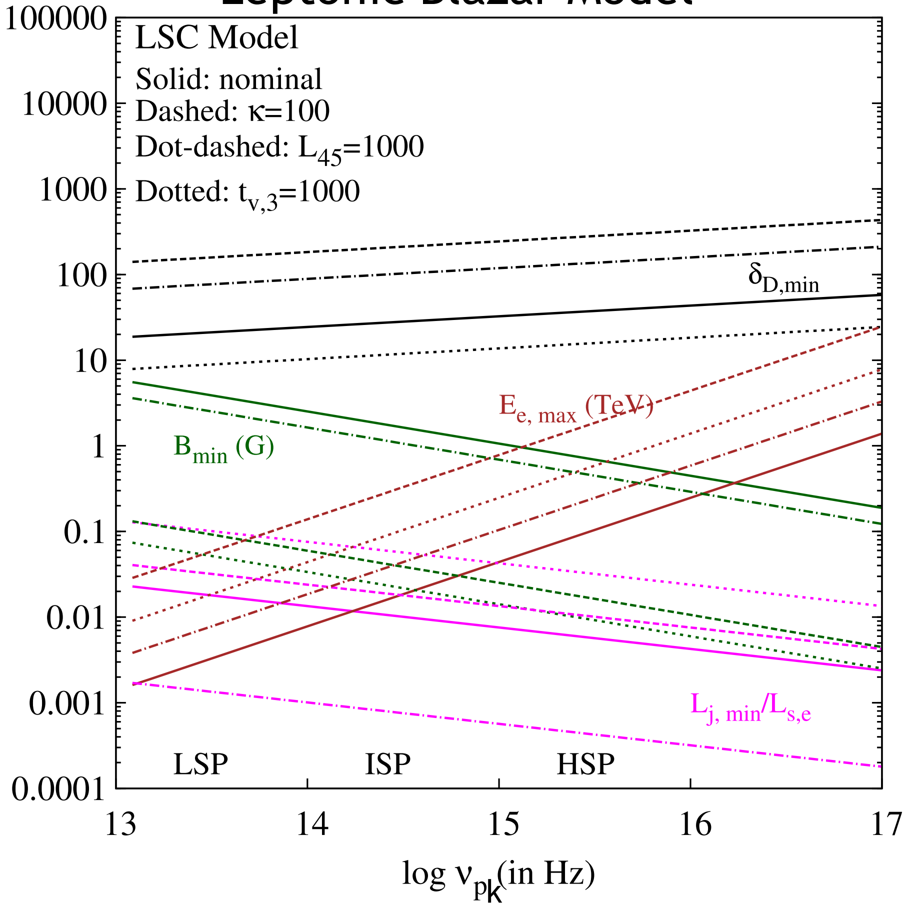

Lepto-Hadronic Synchrotron Blazar Model

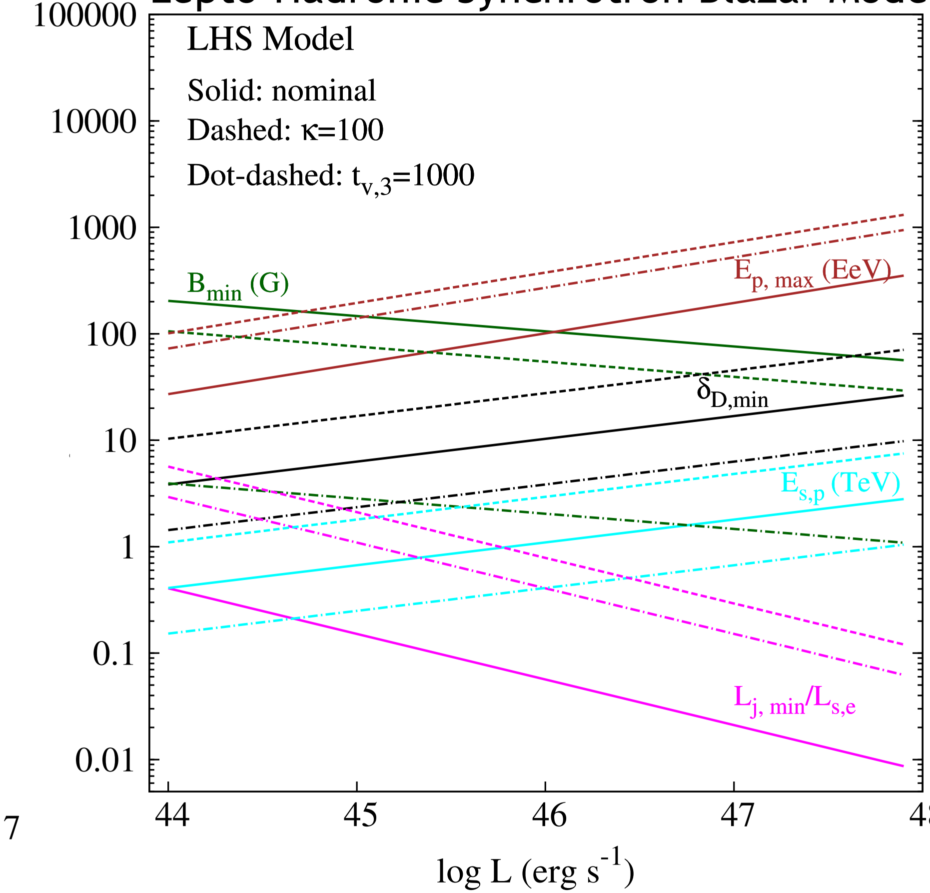

Values of magnetic field and Doppler factor for leptonic model consistent with values derived through trial and error

Comparison of derived properties with numerical calculations

Numerical calculation of jet power as a function of Doppler factor and B’

Leptonic Blazar Model $\quad L_{45} = t_{v,3} = \kappa = 1 \quad$ Lepto-Hadronic Blazar Model

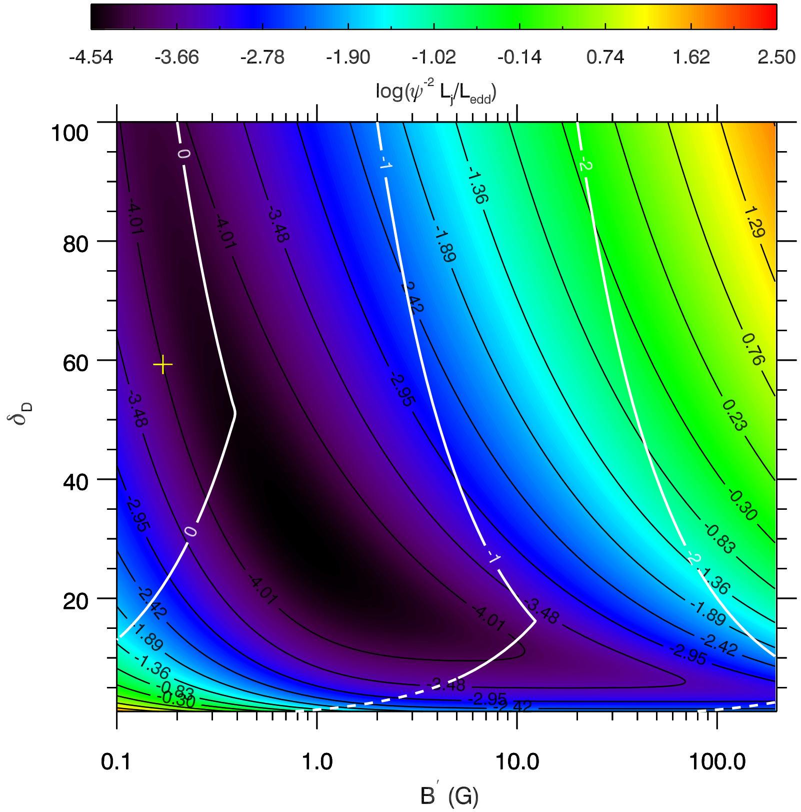

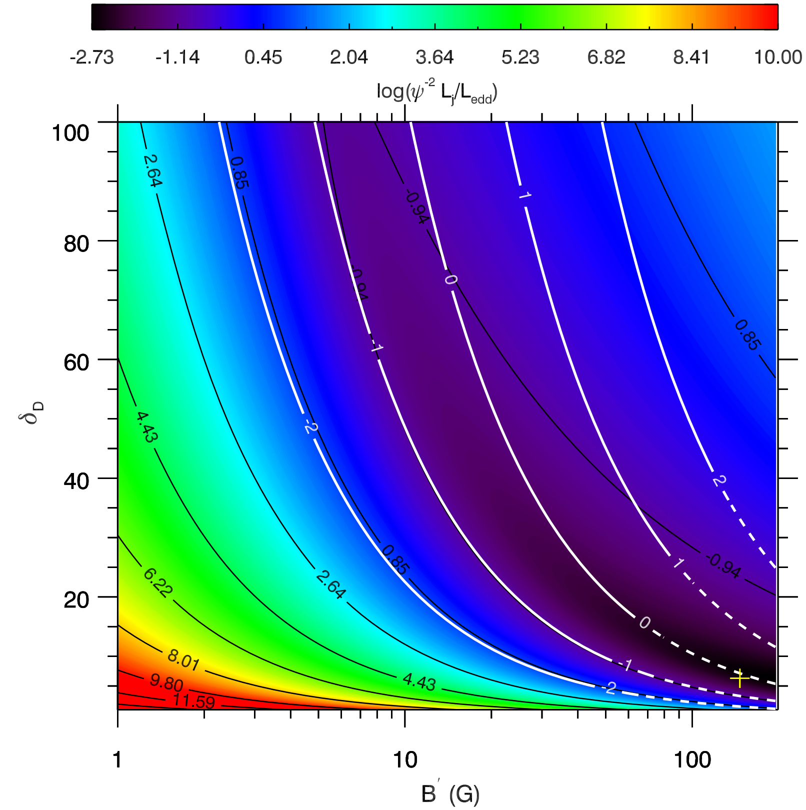

$$\psi^{-2}\frac{L_{j,\min}^{\rm LSC}}{L_{\rm Edd}} \cong 1.4\times 10^{-5}\kappa^{1/8}t_{v,3}^{1/4}L_{45}^{5/8}M_9^{-1}\epsilon_{-3}^{-1/4}$$

$$\psi^{-2}\frac{L_{j,\min}^{\rm LHS}}{L_{\rm Edd}} \cong 10^{-3}(\boldsymbol{\eta}\ \kappa t_{v,3}L_{45}L_{\gamma,45})^{2/7}M_9^{-1}$$

Energetics excessive for FSRQs (but not BL Lacs) for hadronic synchrotron model

BL Lacs remain favored candidate UHECR sources

UHECRs: Luminosity density of blazars from Fermi data

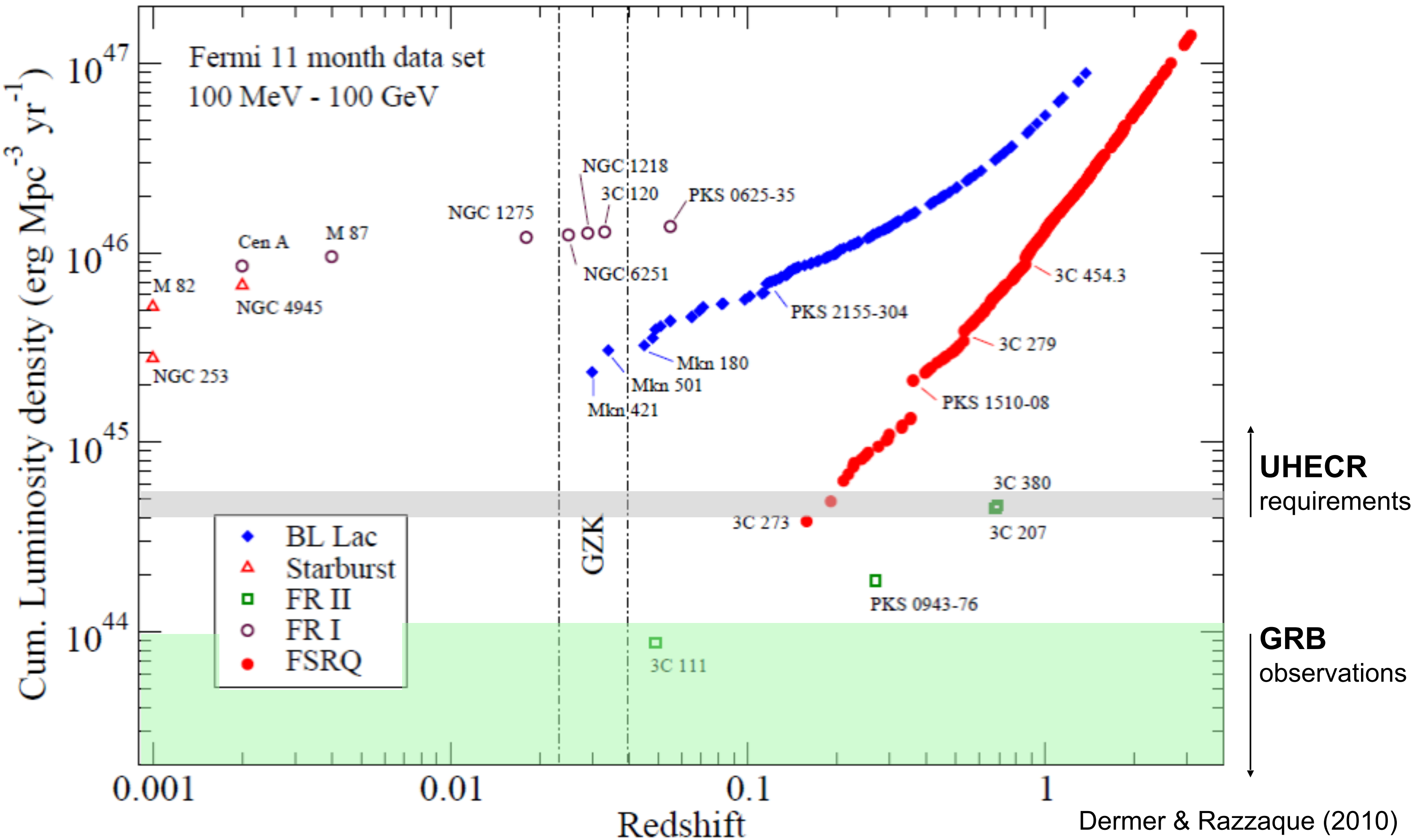

Dermer & Razzaque (2010)

Summary

Outlined two new approaches to blazar modelling:

1) **Near-equipartition approach using log-parabola function for electron energy distribution**
2) **Analysis based on minimizing jet power**

For 1), explains the spectral index diagrams and makes predictions for leptonic models correlating widths of synchrotron component and Compton components: but spectral modelling shows some systems are far from equipartition

For 2), strong magnetic fields B >100 G are found for the LHS model with variability times =10^3 s, in accord with highly magnetized, reconnection-driven jet models. Proton synchrotron models of >100 GeV radiation can be sub-Eddington, but models of GeV radiation in FSRQs require excessive power

1) **Method to determine hadronic content from accurate synchrotron and γ-ray SEDs**
2) **Energetics rules out hadronic synchrotron model for FSRQs but not BL Lacs, consistent with BL Lacs being the sources of the UHECR**